

Origin and Resummation of Threshold Logarithms in the Lattice QCD Calculations of PDFs

Xiang Gao

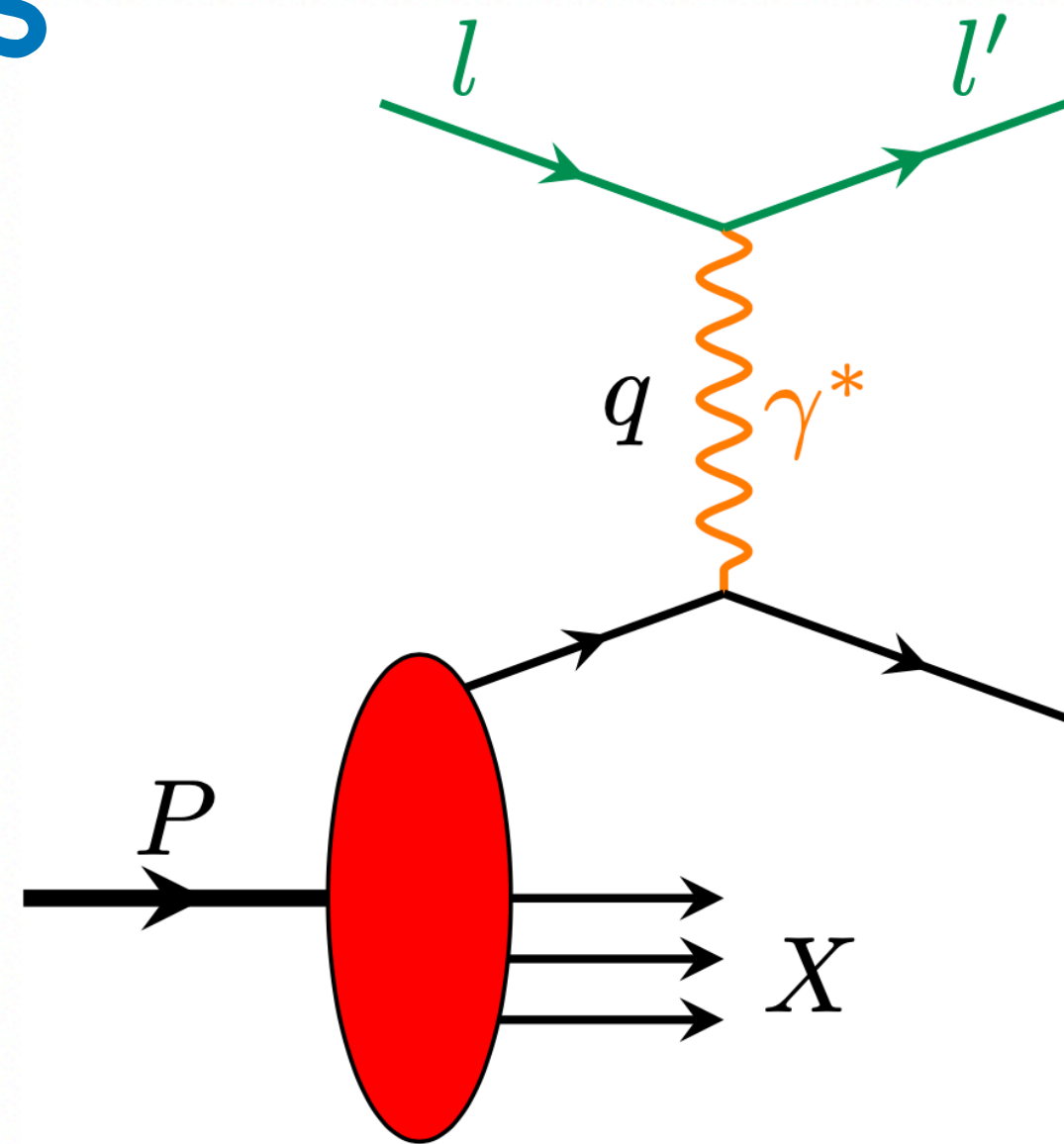
Argonne National Laboratory

Based on **Phys.Rev.D 103 (2021) 9, 094504** with Kyle Lee,
Swagato Mukherjee, Charles Shugert, and Yong Zhao

LaMET 2022, Dec 1 – 3, Chicago

Parton distribution functions

DIS



Non-perturbative PDFs

$$\sigma = \sum_i f_i(x, Q^2) \otimes \sigma \{eq_i(xP) \rightarrow eq_i(xP + q)\}$$

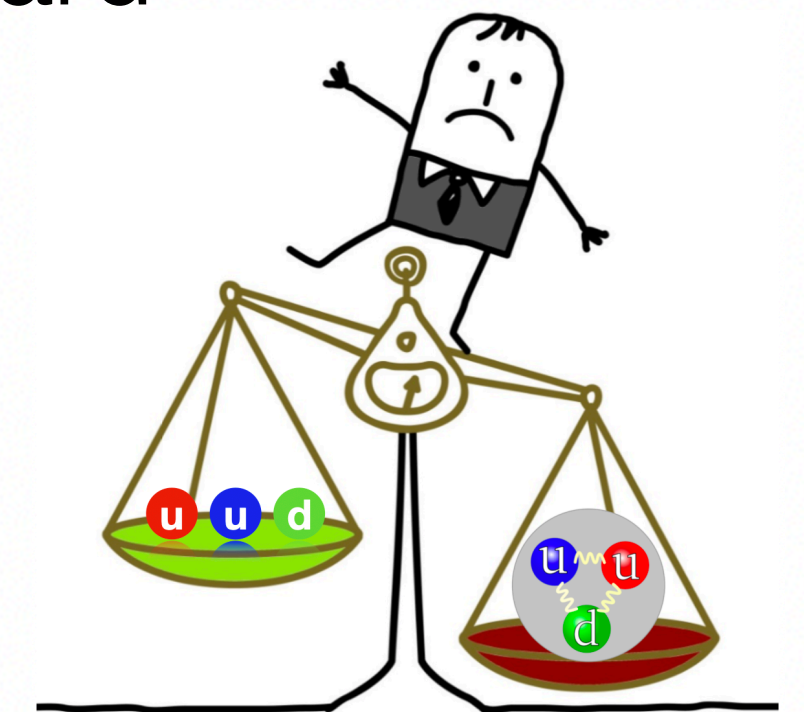
Perturbative parton process

Hadron Structure and Tomography:

- How hadrons are built.
- Mass and spin decomposition of hadron.

High-energy phenomenology:

- Standard Model backgrounds.
- Higgs physics and search for physics beyond the Standard Model.



Large momentum effective theory (LaMET)

Quasi-PDFs Factorization

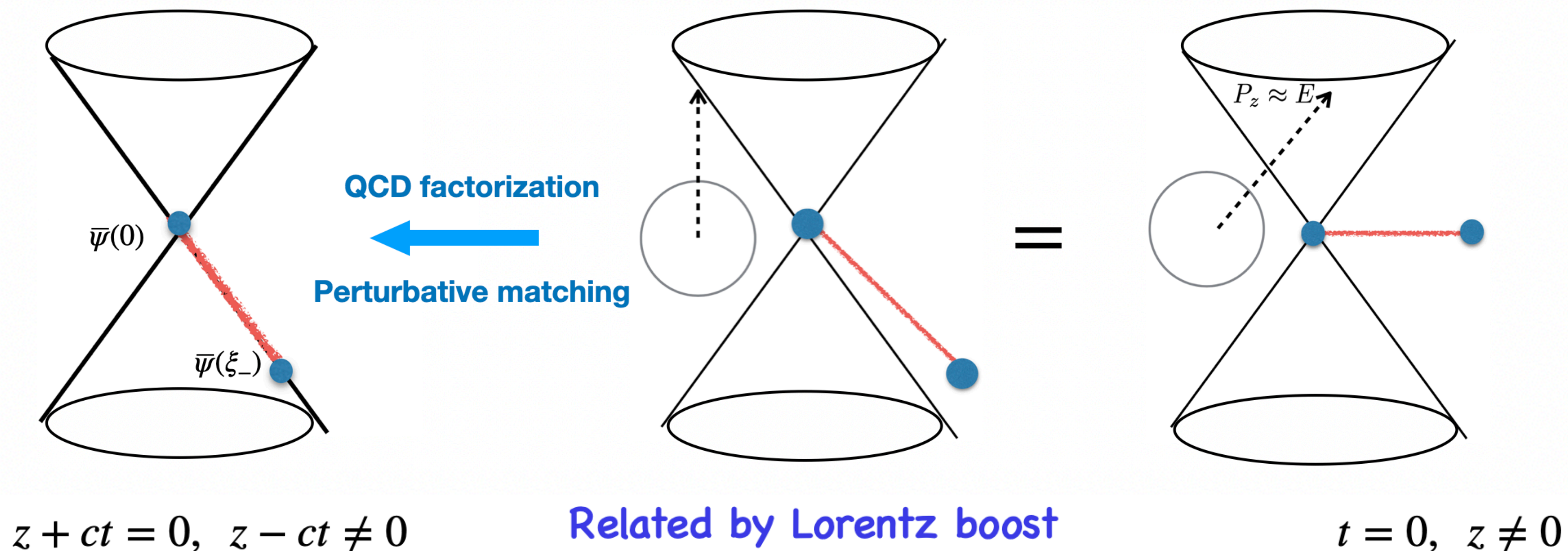
IR must cancel

$$\tilde{q}(x, P_z) = q(x, \mu) + \alpha_s(\mu)(\tilde{q}^{(1)}(x, P_z, \mu) - q^{(1)}(x, \mu))$$

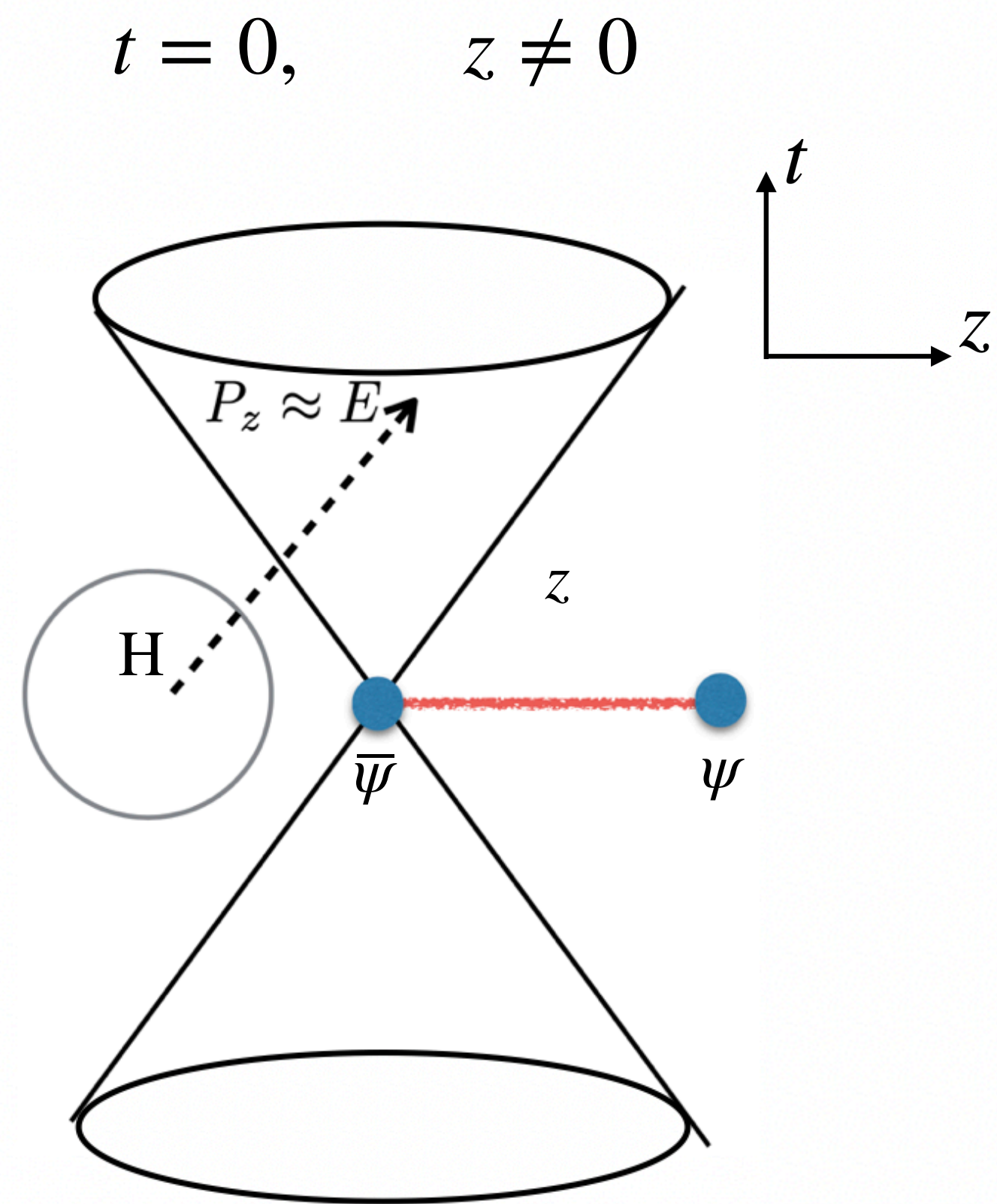
$$= \int \frac{dy}{|y|} C\left(\frac{x}{y}, \frac{\mu}{yP_z}\right) q(y, \mu) + \mathcal{O}\left(\frac{\Lambda_{QCD}^2}{x^2 P_z^2}, \frac{\Lambda_{QCD}^2}{(1-x)P_z^2}\right)$$

- X. Ji, PRL 110 (2013); SCPMA57 (2014);
- X. Xiong, X. Ji, et al, PRD 90 (2014);
- Y.-Q. Ma, et al, PRD98 (2018), PRL 120 (2018);
- T. Izubuchi, X. Ji, et al PRD98 (2018).
- X. Ji, Y. Zhao, et al, RMP 93 (2021).

large P_z is essential



Pseudo PDF / short distance factorization



quasi-PDF matrix elements

$$\langle P | \tilde{O}_\Gamma(z, \epsilon) | P \rangle$$

$$\tilde{O}_\Gamma(z, \epsilon) = \bar{\psi}(0) \Gamma W_{\hat{z}}(0, z) \psi(z)$$

Short-distance factorization:

$$h^R(\lambda, z^2, \mu) = h^R(z, P_z, \mu)$$

$$= \int_{-1}^1 d\alpha \mathcal{C}(\alpha, \mu^2 z^2) \int_{-1}^1 dy e^{-iy\alpha\lambda} q(y, \mu) + \mathcal{O}(z^2 \Lambda_{QCD}^2)$$

Perturbative kernel

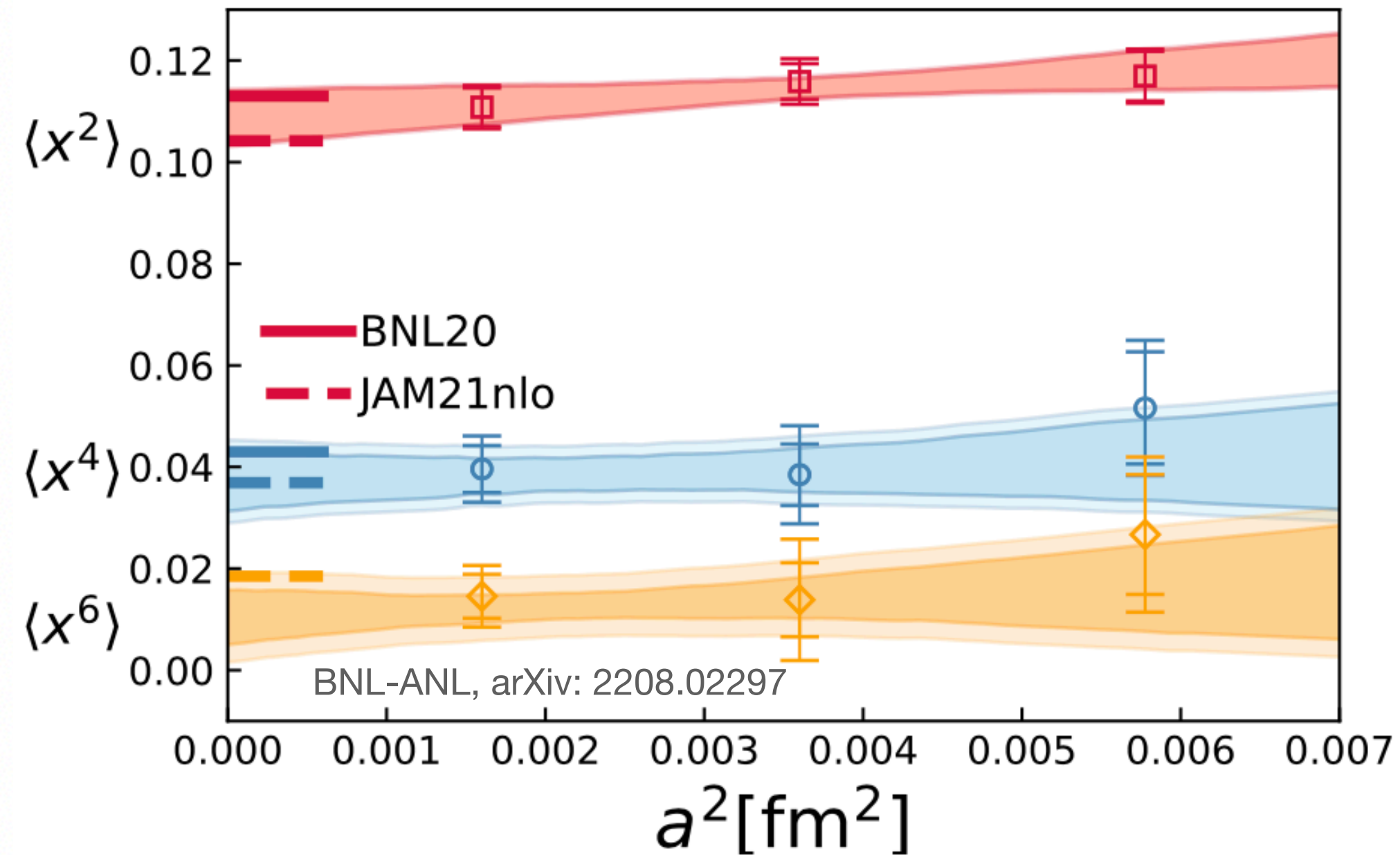
$$\lambda = zP_z$$

- The perturbative matching is valid in short range of z .
- The information that lattice data contains is limited by the range of **finite** $\lambda = zP_z$.

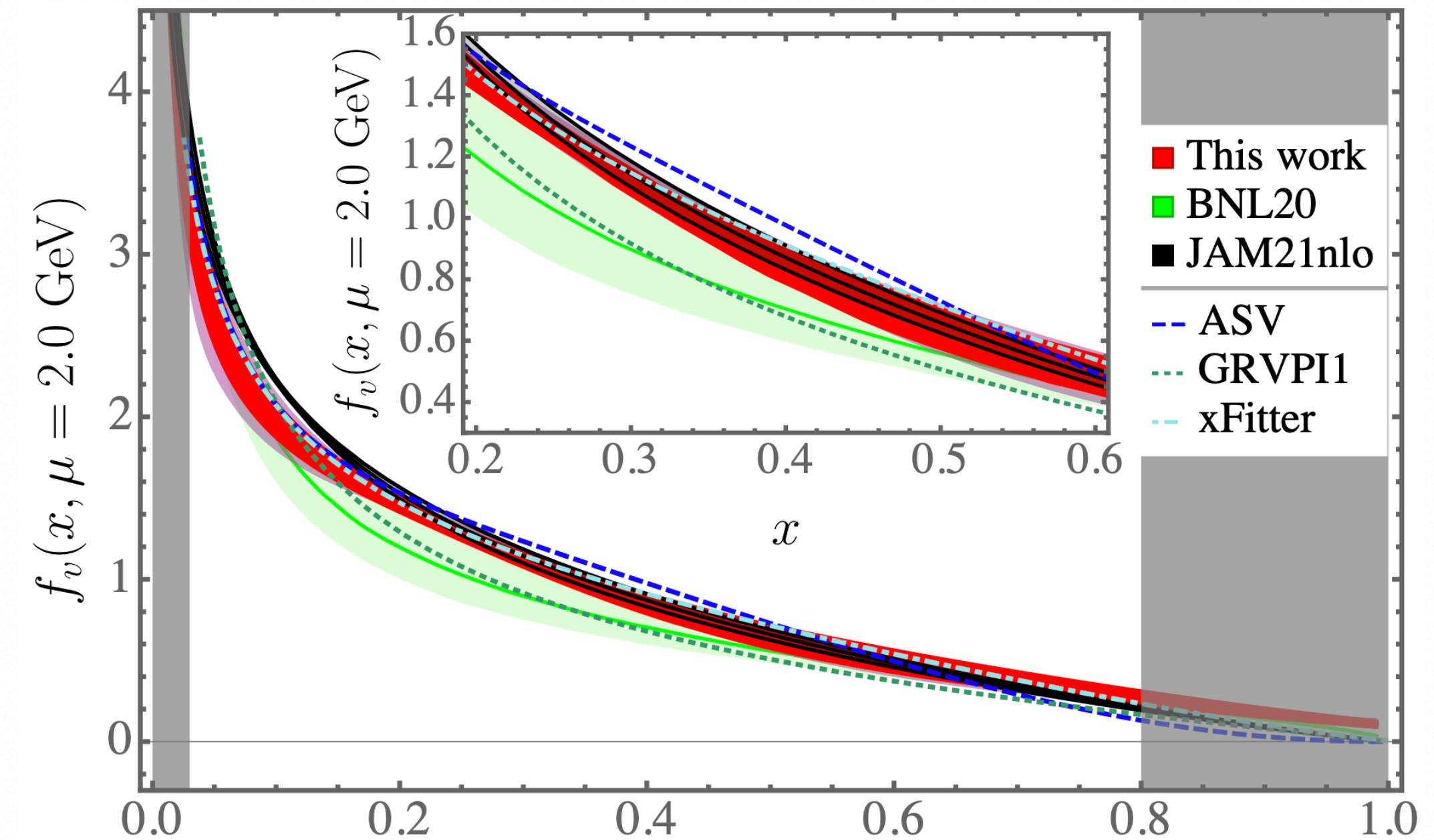
- V. Braun et al., EPJC 55 (2008)
- A. V. Radyushkin et al., PRD 96 (2017)
- Y. Ma et al., PRL 120 (2018)
- T. Izubuchi et al., PRD 98 (2018)

Pion valence quark PDF: fixed order

Moments of pion valence quark PDF



Pion valence quark PDF

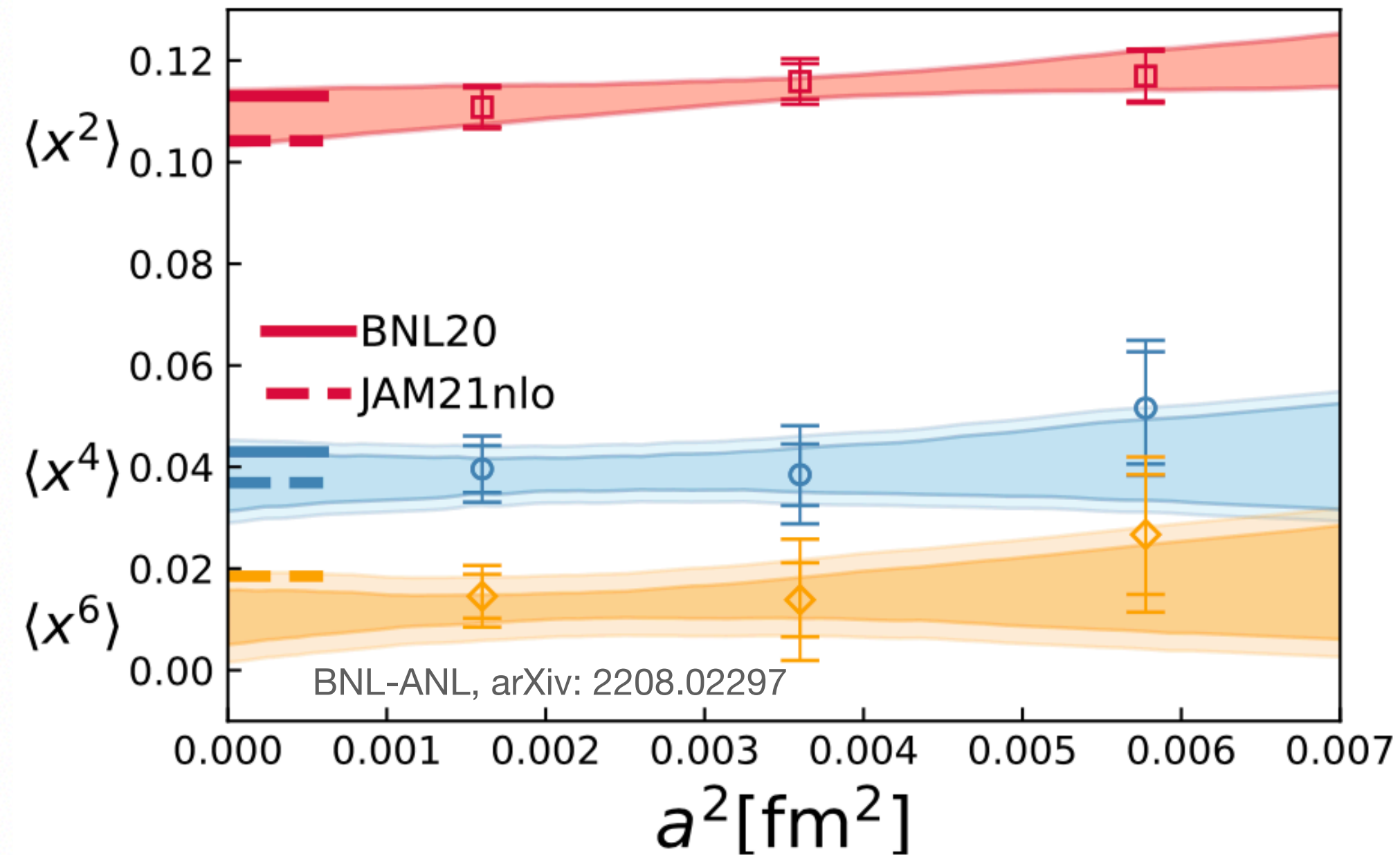


• BNL-ANL, PRL 128 (2022) 14, 142003

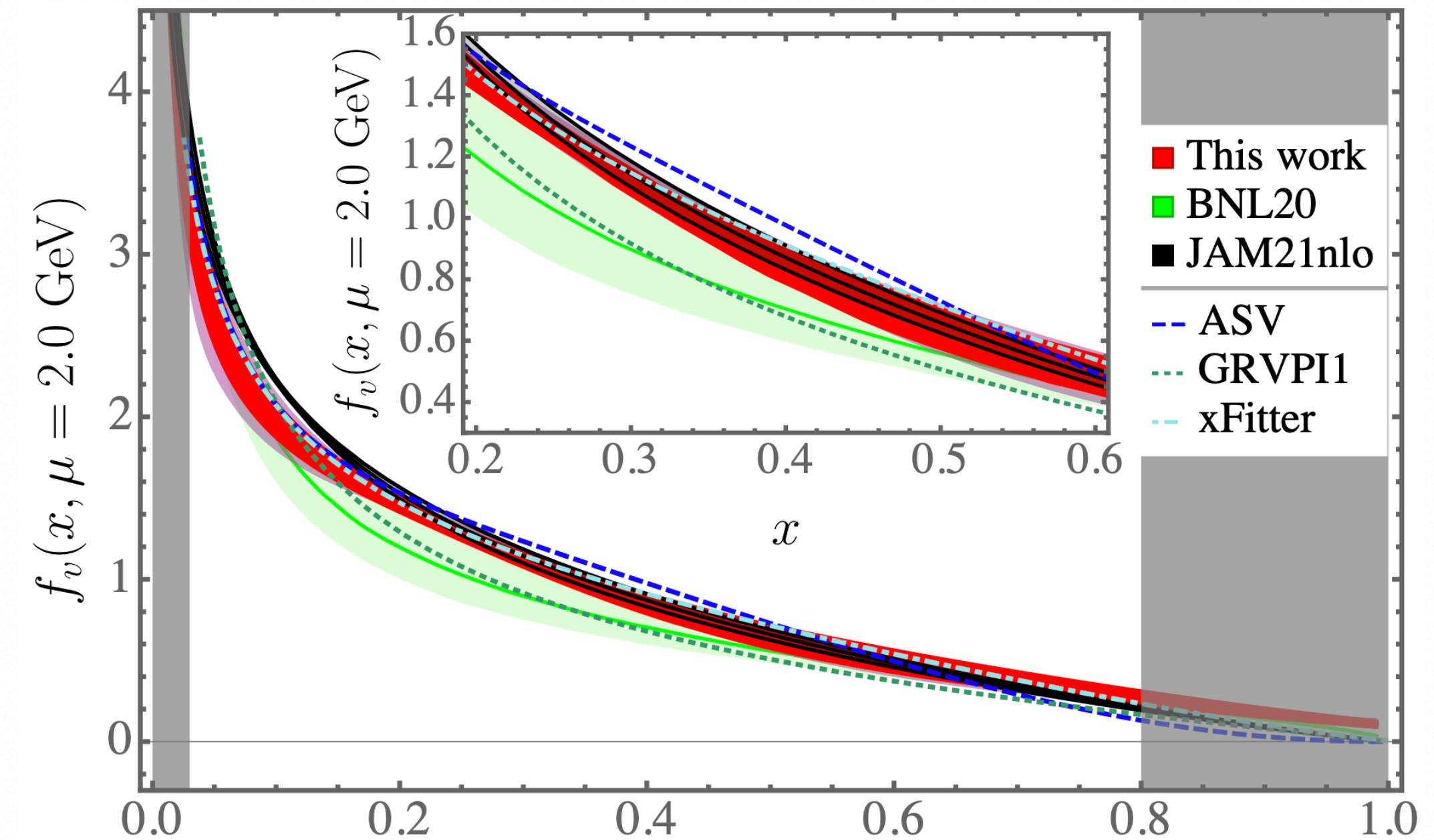
- Lattice prediction of pion valence PDF show good agreement with most recent Global analysis from JAM, xFitter.

Pion valence quark PDF: fixed order

Moments of pion valence quark PDF



Pion valence quark PDF



• BNL-ANL, PRL 128 (2022) 14, 142003

Improvement:

- Higher statistics.
- Lattice artifacts: smaller lattice spacing, chiral fermion calculations.
- Power correction: larger momentum.
- Perturbative matching: higher order, **resummation**.
- ...

Large momentum effective theory (LaMET)

Quasi-PDFs Factorization:

$$\tilde{q}(x, P_z) = \int \frac{dy}{|y|} C\left(\frac{x}{y}, \frac{\mu}{yP_z}\right) q(y, \mu) + \mathcal{O}\left(\frac{\Lambda_{QCD}^2}{x^2 P_z^2}, \frac{\Lambda_{QCD}^2}{(1-x)P_z^2}\right)$$

One-loop matching:

$$C^{(1)}\left(\xi, \frac{\mu}{|y|P_z}\right) = \frac{\alpha_s C_F}{2\pi} \delta(1-\xi) \left[\frac{3}{2} \ln \frac{\mu^2}{4y^2 P_z^2} - \frac{5}{2} \right]$$

$$+ \frac{\alpha_s C_F}{2\pi} \begin{cases} \left(\frac{1+\xi^2}{1-\xi} \ln \frac{\xi}{\xi-1} + 1 \right)_+ & \xi > 1 \\ \frac{1+\xi^2}{1-\xi} \left[-\ln \frac{\mu^2}{4y^2 P_z^2} - \ln \frac{\xi}{1-\xi} - 1 \right]_+ & 0 < \xi < 1 \\ \left(-\frac{1+\xi^2}{1-\xi} \ln \frac{-\xi}{1-\xi} - 1 \right)_+ & \xi < 0 \end{cases}$$

DGLAP evolution

- X. Ji, Y. Zhao, et al, RMP 93 (2021).
- Y. Su et al, arXiv: 2209.01236

$$\frac{dC^{(1)}\left(\xi, \frac{\mu}{yP_z}\right)}{d \ln(yP_z)} = \frac{\alpha_s}{\pi} \left[P_{qq}^{(0)}(\xi) - \frac{3}{2}(1-\xi) \right]$$

Large momentum effective theory (LaMET)

Quasi-PDFs Factorization:

$$\tilde{q}(x, P_z) = \int \frac{dy}{|y|} C\left(\frac{x}{y}, \frac{\mu}{yP_z}\right) q(y, \mu) + \mathcal{O}\left(\frac{\Lambda_{QCD}^2}{x^2 P_z^2}, \frac{\Lambda_{QCD}^2}{(1-x)P_z^2}\right)$$

One-loop matching:

$$C^{(1)}\left(\xi, \frac{\mu}{|y|P_z}\right) = \frac{\alpha_s C_F}{2\pi} \delta(1-\xi) \left[\frac{3}{2} \ln \frac{\mu^2}{4y^2 P_z^2} - \frac{5}{2} \right]$$

$$+ \frac{\alpha_s C_F}{2\pi} \begin{cases} \left(\frac{1+\xi^2}{1-\xi} \ln \frac{\xi}{\xi-1} + 1 \right)_+ & \xi > 1 \\ \frac{1+\xi^2}{1-\xi} \left[-\ln \frac{\mu^2}{4y^2 P_z^2} - \ln \frac{\xi}{1-\xi} - 1 \right]_+ & 0 < \xi < 1 \\ \left(-\frac{1+\xi^2}{1-\xi} \ln \frac{-\xi}{1-\xi} - 1 \right)_+ & \xi < 0 \end{cases}$$

Threshold logarithms

- X. Gao, et al, Phys.Rev.D 103 (2021) 9

$$\lim_{\substack{x,y \rightarrow 1 \\ \xi \rightarrow 1}} C^{(1)}\left(\xi, \frac{\mu}{|y|p^z}\right)$$

$$\sim \frac{\alpha_s C_F}{2\pi} \left[\frac{2 \ln |1-\xi|}{|1-\xi|} - \frac{2}{(1-\xi)} \ln \frac{\mu^2}{4p_z^2} + \frac{3}{2|1-\xi|} \right]_+$$

$$\frac{2}{|1-\xi|} \ln \frac{|1-\xi| P_z^2}{\mu^2}$$

$\xi \rightarrow 1$ approaching Landau pole

The pseudo distribution

Short-distance Factorization:

$$h^R(\lambda, z^2, \mu) = \int_{-1}^1 d\alpha \mathcal{C}(\alpha, \mu^2 z^2) \int_{-1}^1 dy e^{-iy\alpha\lambda} q(y, \mu) + \mathcal{O}(z^2 \Lambda_{QCD}^2)$$

One-loop matching:

$$\begin{aligned} \mathcal{C}^{(1)}(\alpha, z^2 \mu^2) = & \delta(1 - \alpha) \frac{\alpha_s C_F}{2\pi} \left[\frac{3}{2} \ln \frac{z^2 \mu^2 e^{2\gamma_E}}{4} + \frac{5}{2} \right] \\ & + \frac{\alpha_s C_F}{2\pi} \left\{ \left(\frac{1 + \alpha^2}{1 - \alpha} \right)_+ \left[-\ln \frac{z^2 \mu^2 e^{2\gamma_E}}{4} - 1 \right] \right. \\ & \left. - \left(\frac{4 \ln(1 - \alpha)}{1 - \alpha} \right)_+ + 2(1 - \alpha)_+ \right\} \theta(\alpha) \theta(1 - \alpha) \end{aligned}$$

DGLAP evolution

- A. V. Radyushkin, Phys.Lett.B 781 (2018).
- X. Ji, Y. Zhao, et al, RMP 93 (2021).
- Y. Su et al, arXiv: 2209.01236

$$\frac{d\mathcal{C}(\alpha, \mu^2 z^2)}{d \ln z^2} = \frac{\alpha_s}{2\pi} \left[-P_{qq}^{(0)}(\alpha) - \frac{3}{2}(1 - \alpha) \right]$$

The pseudo distribution

Short-distance Factorization:

$$h^R(\lambda, z^2, \mu) = \int_{-1}^1 d\alpha \mathcal{C}(\alpha, \mu^2 z^2) \int_{-1}^1 dy e^{-iy\alpha\lambda} q(y, \mu) + \mathcal{O}(z^2 \Lambda_{QCD}^2)$$

One-loop matching:

$$\begin{aligned} \mathcal{C}^{(1)}(\alpha, z^2 \mu^2) = & \delta(1 - \alpha) \frac{\alpha_s C_F}{2\pi} \left[\frac{3}{2} \ln \frac{z^2 \mu^2 e^{2\gamma_E}}{4} + \frac{5}{2} \right] \\ & + \frac{\alpha_s C_F}{2\pi} \left\{ \left(\frac{1 + \alpha^2}{1 - \alpha} \right)_+ \left[-\ln \frac{z^2 \mu^2 e^{2\gamma_E}}{4} - 1 \right] \right. \\ & \left. - \left(\frac{4 \ln(1 - \alpha)}{1 - \alpha} \right)_+ + 2(1 - \alpha)_+ \right\} \theta(\alpha) \theta(1 - \alpha) \end{aligned}$$

Threshold logarithms

- X. Gao, et al, Phys.Rev.D 103 (2021) 9

$$\begin{aligned} \lim_{\alpha \rightarrow 1} \mathcal{C}^{(1)}(\alpha, z^2 \mu^2) \\ \sim \frac{\alpha_s C_F}{2\pi} \left[\frac{4 \ln(1 - \alpha)}{1 - \alpha} - \frac{2}{(1 - \alpha)} \ln \frac{z^2 \mu^2 e^{2\gamma_E}}{4} - \frac{2}{1 - \alpha} \right]_+ \\ \quad \quad \quad \frac{2}{1 - \alpha} \ln \frac{4e^{-2\gamma_E}}{(1 - \alpha)^2 z^2 \mu^2} \end{aligned}$$

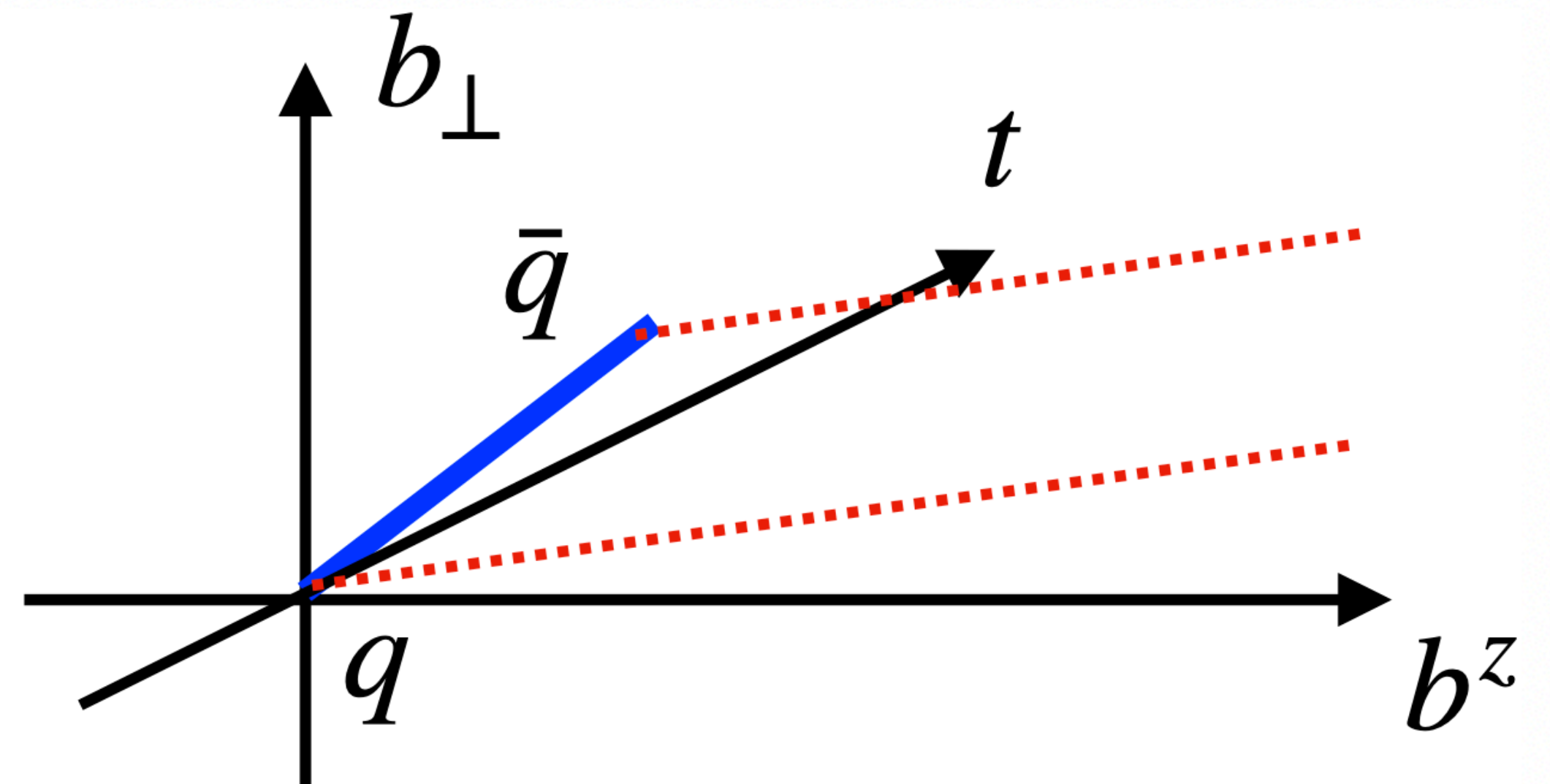
$\alpha \rightarrow 1$ approaching UV fixed point

11 Origin of threshold logarithms

3D momentum distribution

$$\tilde{q}(x, \vec{k}_\perp, P^z) = \frac{1}{2P^0} \int \frac{db_z d^2\vec{b}_\perp}{(2\pi)^3} e^{i\vec{k}_\perp \cdot \vec{b}_\perp + ib_z(xP^z)} \\ \times \langle P | \bar{\psi}(b) W(b, 0) \gamma^t \psi(0) | P \rangle$$

- **Straight-line** gauge link
- Different from normal TMD distribution with a staple shaped gauge link



12 Origin of threshold logarithms

3D momentum distribution

$$\tilde{q}(x, \vec{k}_\perp, P^z) = \frac{1}{2P^0} \int \frac{db_z d^2\vec{b}_\perp}{(2\pi)^3} e^{i\vec{k}_\perp \cdot \vec{b}_\perp + ib_z(xP^z)} \\ \times \langle P | \bar{\psi}(b) W(b,0) \gamma^t \psi(0) | P \rangle$$

• Relation to the quasi-PDF

$$\int d^2\vec{k}_\perp \tilde{q}(x, \vec{k}_\perp, P^z) = \tilde{q}(x, P^z)$$

or

$$\lim_{b_\perp \rightarrow 0} \tilde{q}(x, \vec{b}_\perp, P^z) = \tilde{q}(x, P^z)$$

• Relation to the pseudo-PDF

$$\frac{1}{2P^0} \langle P | \bar{\psi}(b) W(b,0) \gamma^t \psi(0) | P \rangle = h(P \cdot b, b^2)$$

spacial correlator

In the limit of $P_z \rightarrow \infty$, $b_z \rightarrow 0$, $\lambda = P_z b_z$ finite

$$\lim_{P^z \rightarrow \infty} \tilde{q}(x, \vec{b}_\perp, P^z) \\ = \int_{-\infty}^{\infty} \frac{d\lambda}{2\pi} e^{i\lambda x} \tilde{h}_{\gamma^t}(\lambda, -b^2 = \vec{b}_\perp^2) \\ = \mathcal{P}(x, \vec{b}_\perp^2)$$

primordial TMD

• A. V. Radyushkin, Phys.Rev.D 96 (2017)

$$\vec{b}_\perp^2 = z^2$$

Origin of threshold logarithms

• Quasi-PDF

$$\frac{2}{|1 - \xi|} \ln \frac{|1 - \xi| P_z^2}{\mu^2}$$

$\xi \rightarrow 1$ approaching Landau pole

Since k_\perp is integrated over, the limit $x \rightarrow 1$ includes contributions from both hard and soft transverse momentum modes, with the latter being sensitive to IR physics.

$$\int d^2\vec{k}_\perp \tilde{q}(x, \vec{k}_\perp, P^z) = \tilde{q}(x, P^z)$$

• Pseudo-PDF

$$\frac{2}{1 - \alpha} \ln \frac{4e^{-2\gamma_E}}{(1 - \alpha)^2 z^2 \mu^2}$$

$\alpha \rightarrow 1$ approaching UV fixed point

Since pPDF corresponds to the primordial TMD, the emitted gluon remains off-shell with virtual mass k_\perp in the limit of $x \rightarrow 1$. In coordinate space, small b_\perp corresponds to large k_\perp , so the gluon is in the UV region.

$$\lim_{P^z \rightarrow \infty} \tilde{q}(x, \vec{b}_\perp, P^z)$$

Threshold resummation at NLL accuracy

In the Mellin-moment space (OPE)

$$a_N(\mu) = \int_{-1}^1 dy y^N q(y, \mu)$$

$$\tilde{h}_{\gamma^t}(\lambda, z^2 \mu^2) = \sum_{N=0}^{\infty} \frac{(-i\lambda)^N}{N!} C_N(\alpha_s(\mu), z_0^2 \mu^2) a_N(\mu) + \dots$$

- At NLO

$$\begin{aligned} C_N^{\text{NLO}} &= \int_0^1 dw w^N \mathcal{C}^{\text{NLO}}(w, z^2 \mu^2) \\ &= \frac{\alpha_s(\mu) C_F}{2\pi} \left[\left(\frac{3+2N}{2+3N+N^2} + 2H_N \right) \ln(z_0^2 \mu^2) \right. \\ &\quad \left. + \frac{5+2N}{2+3N+N^2} + 2(1 - H_N)H_N - 2H_N^{(2)} \right] \end{aligned}$$

- The threshold limit corresponds to $N \rightarrow \infty$

$$\lim_{N \rightarrow \infty} C_N^{\text{NLO}} = \frac{\alpha_s(\mu) C_F}{2\pi} \left[2 \ln N' \ln(z_0^2 \mu^2) - 2 \ln^2 N' + 2 \ln N' - \frac{\pi^2}{3} \right],$$

$$\begin{array}{ll} \alpha_s \ln^2 N', & \alpha_s \ln N' \\ \text{LL} & \text{NLL} \end{array} \quad N' = Ne^{\gamma_E}$$

Threshold resummation at NLL accuracy

Using the standard technique of threshold resummation

$$\ln C_N^{\text{NLL}} = \int dx \frac{x^{N-1} - 1}{1-x} \left[\int_{\mu^2}^{\frac{(1-x)^{-2}}{z_0^2}} \frac{dk^2}{k^2} A(\alpha_s(k^2)) + B(\alpha_s((1-x)^{-2}/z_0^2)) \right]$$

$$A(\alpha_s) = A^{(0)}a_s + A^{(1)}a_s^2 + \dots, \quad B(\alpha_s) = B^{(0)}a_s + B^{(1)}a_s^2 + \dots$$

- **Leading logarithm (LL)**

$$A^{(0)} = -B^{(0)} = 2C_F$$

- **For NLL which neglects $\mathcal{O}(\alpha_s^2 \ln N')$ terms**

$$A^{(1)} = 2C_F \left[C_A \left(\frac{67}{18} - \frac{\pi^2}{6} \right) - \frac{10}{9} n_f T_F \right]$$

- **DGLAP evolution may also be considered**

$$\left[\frac{\partial}{\partial \ln \mu^2} + \beta(a_s(\mu)) \frac{\partial}{\partial a_s} - \gamma_N \right] C_N = 0$$

Threshold resummation at NLL accuracy

- **NLL** threshold resummation + **LL** DGLAP evolution (evo)

$$C_N^{\text{NLL+evo}}(\alpha_s(\mu), z_0^2 \mu^2) = C_N^{\text{NLL}}(\alpha_s(z_0^{-1}), 1) \left(\frac{\alpha_s(z_0^{-1})}{\alpha_s(\mu)} \right)^{\frac{\gamma_N^{(0)}}{\beta_0}}$$

$$\ln C_N^{\text{NLL}}(\alpha_s(z_0^{-1}), 1) = -\frac{\pi^2}{3} a_s C_F + \ln N' g_1(\tau, 0) + g_2(\tau, 0)$$

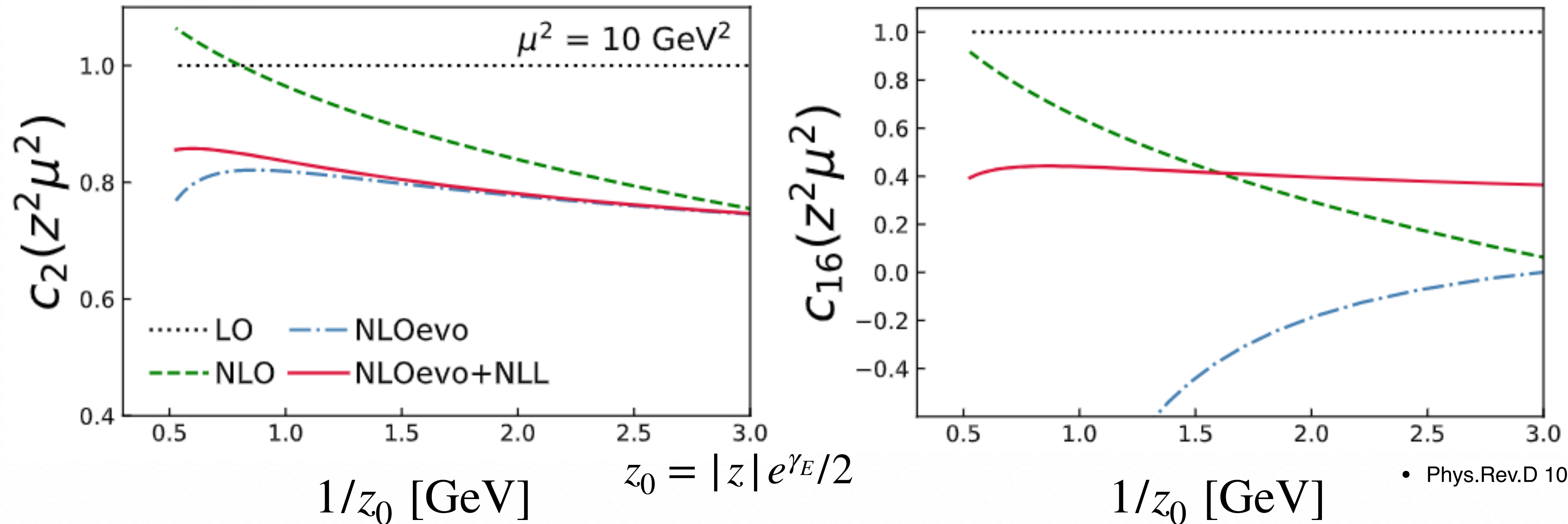
• Phys.Rev.D 103 (2021) 9, 094504

- Using the **inverse Mellin transform**, we can eventually obtain the resummed matching coefficient

$$\mathcal{C}^{\text{NLL+evo}}(w, z^2 \mu^2) = e^{-\frac{\pi^2}{3} a_s C_F} \frac{1}{2\pi i} \int_{C-i\infty}^{C+i\infty} dN w^{-N} \\ \times \exp \left[\ln N' g_1(\tau, 0) + g_2(\tau, 0) \right] \left(\frac{\alpha_s(z_0^{-1})}{\alpha_s(\mu)} \right)^{\frac{\gamma_N^{(0)}}{\beta_0}}$$

Impacts of NLL resummation

The Wilson coefficient at LO, NLO, NLOevo, and NLOevo+NLL accuracy

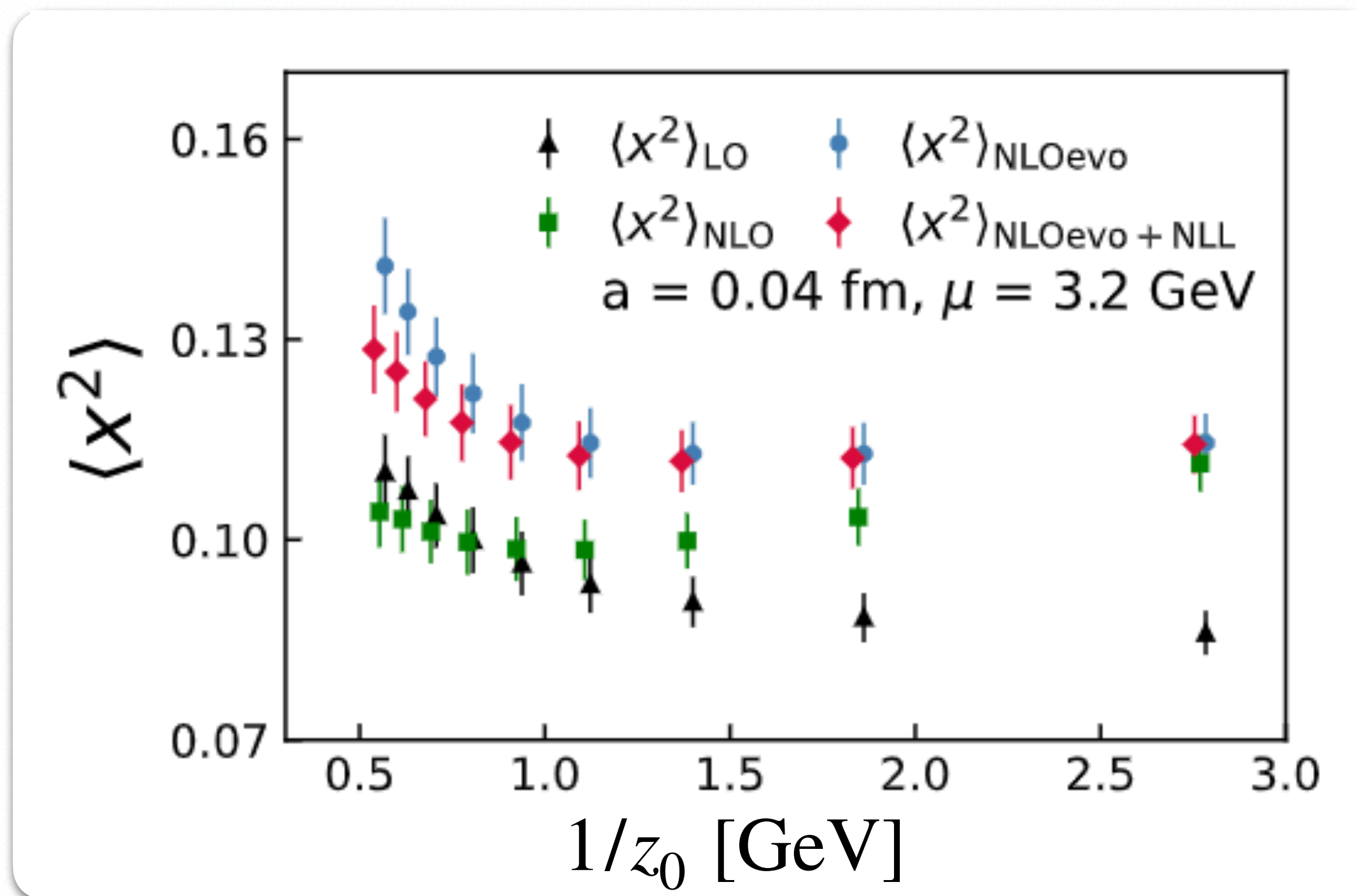


• Phys.Rev.D 103 (2021) 9, 094504

- DGLAP evolution is important when $1/z_0$ is far from μ .
- **Threshold resummation** is necessary for either **large α_s** or **large N**

Impacts of NLL resummation

$\langle x^2 \rangle$ by fitting $a = 0.04$ fm lattice results with pion boosted up to 2.42 GeV

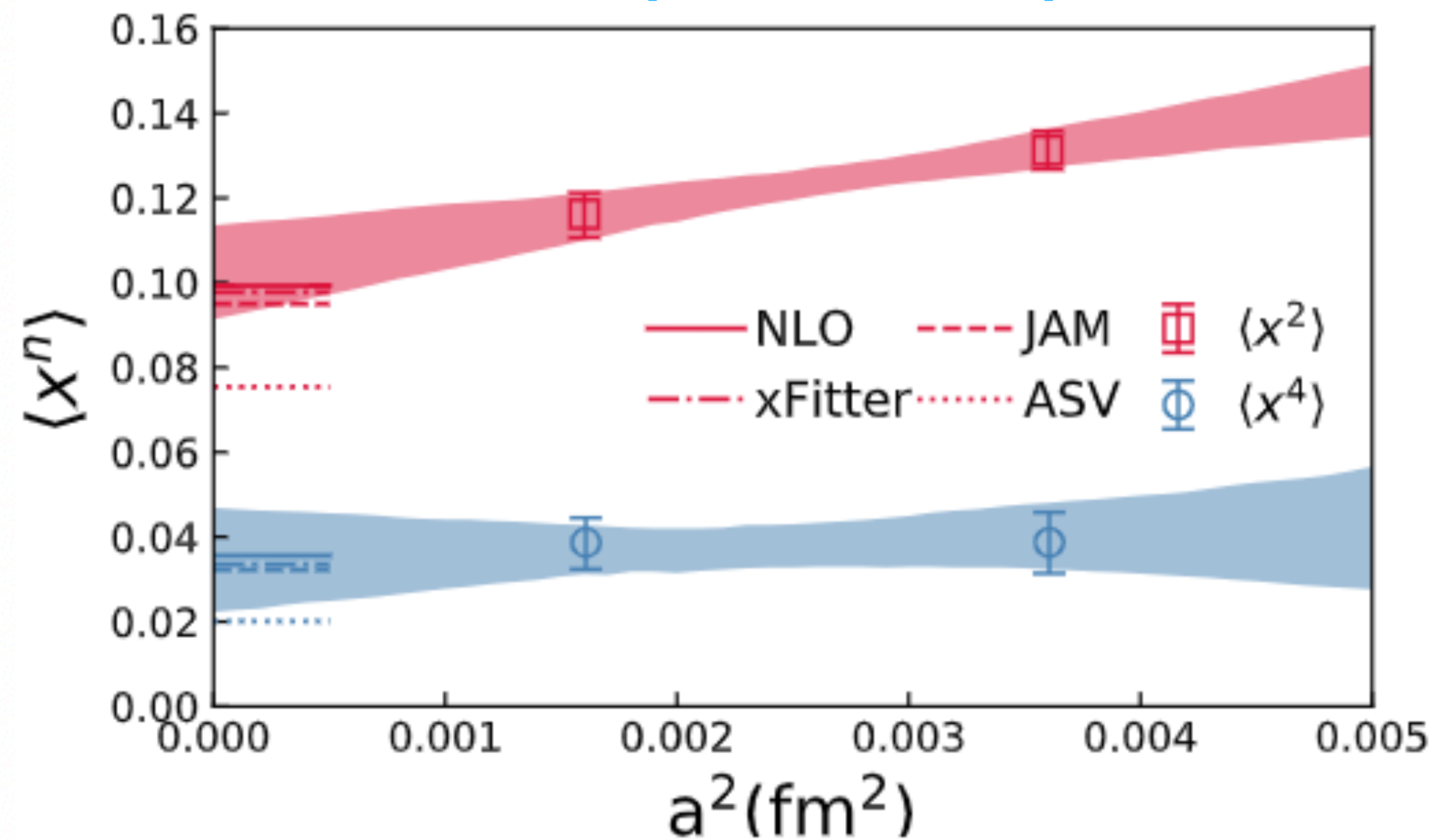


$$z_0 = |z| e^{y_E/2}$$

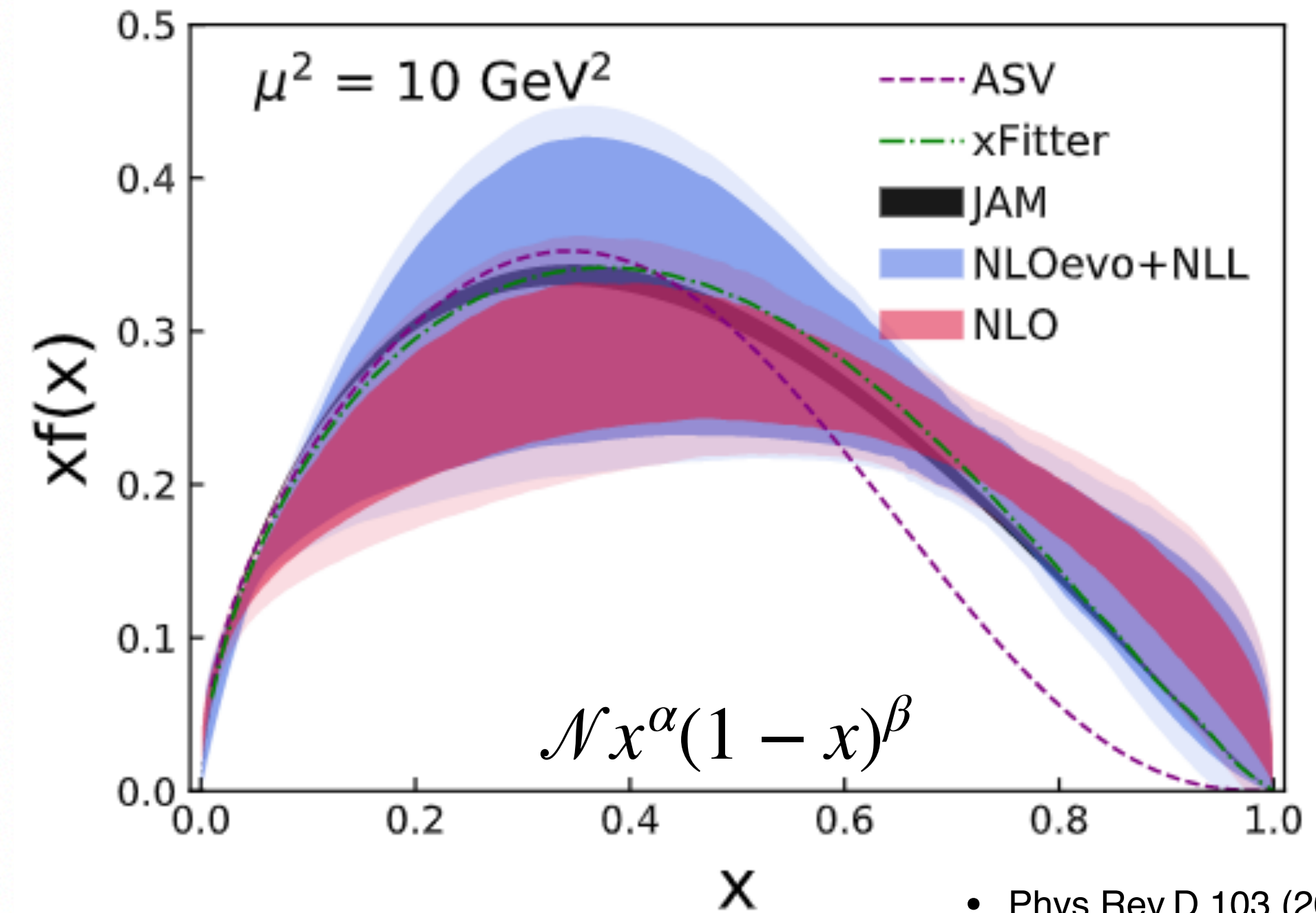
- At **LO** one can clearly observe the z -dependence.
- **Beyond LO**, one can find a plateau indicating that the coefficients can explain the z -dependence.
- **Threshold resummation** slightly improve the plateau.

Impacts of NLL resummation

Moments of pion valence quark PDF



Pion valence quark PDF



• Phys.Rev.D 103 (2021) 9, 094504

- Our current lattice data are only sensitive to the **first few moments**, where threshold resummation has mild impact.
- Situation can be improved if we manage to get more precise data and increase the pion momentum aimed for **higher moments**.

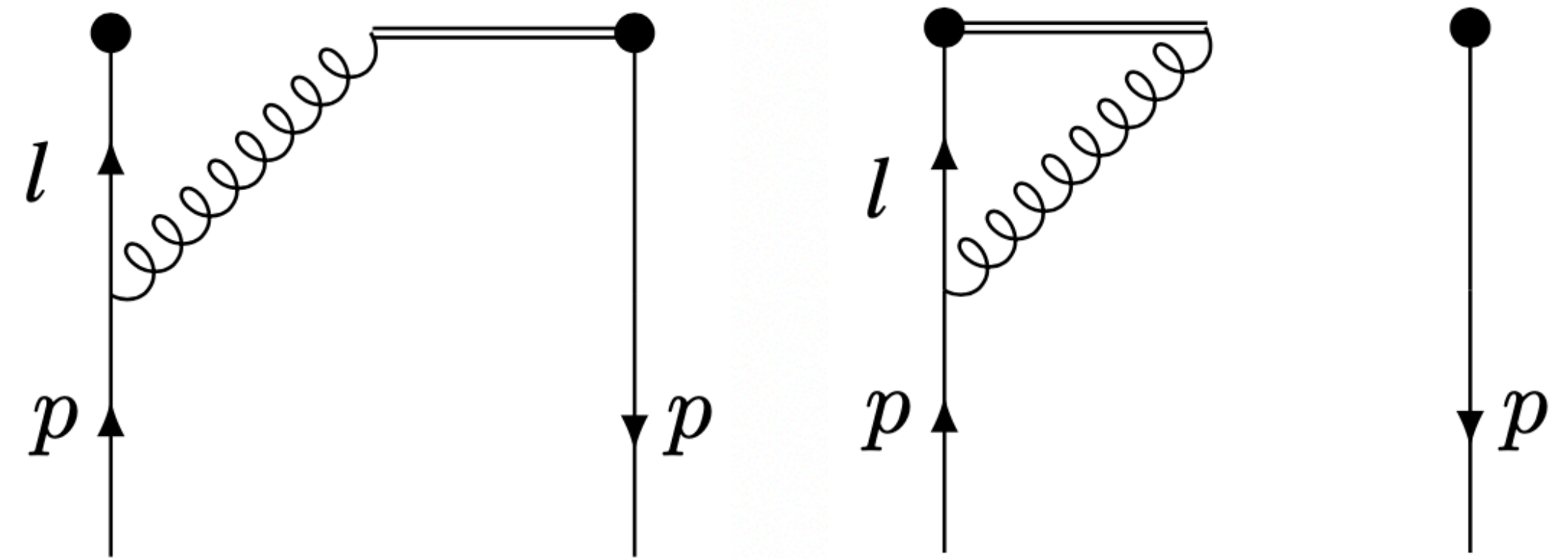
Summary

- Precision lattice calculation of PDFs will require QCD evolution and resummation.
- The origin of threshold logarithms in the quasi-PDF and spatial correlators is identified, and resummed using standard techniques.
- Current lattice data are only sensitive to the lowest moments or finite- x range of the PDF, so the effect of threshold resummation is not significant.
- Threshold resummation will be important for future calculations with larger hadron momenta to study the large- x behavior of the PDF.

21 Origin of threshold logarithms

Leading divergence in the one-loop diagram

$$\begin{aligned} & \tilde{q}_{cs}^{(1)}(x, \vec{k}_\perp, p^z) \\ &= \frac{g^2 \mu^{2\epsilon} C_F}{2(2\pi)^{d-1}} \int_0^1 ds \frac{(1-s)^{2-d}}{\vec{k}_\perp^2} \quad k_t^2 = \vec{k}_\perp^2 / p_z^2 \\ & \times \left[\frac{k_t^2(1+x-2s) + (x-s)^3}{(k_t^2 + (s-x)^2)^{3/2}} - \frac{k_t^2(1+x-2s) + (x-1)^3}{(k_t^2 + (x-1)^2)^{3/2}} \right] \end{aligned}$$



- To obtain the quasi-PDF

$$\begin{aligned} \tilde{q}_{cs}^{(1)}(x, p^z) &= \int d^{d-2} k_\perp \tilde{q}_{cs}^{(1)}(x, \vec{k}_\perp, p^z) \\ &\xrightarrow{x \rightarrow 1^-} -\frac{g^2 C_F}{8\pi^2} \frac{1}{\epsilon} \frac{1 + (1-x)^{-2\epsilon}}{1-x} \left(\frac{\mu^2}{p_z^2} \right)^\epsilon \end{aligned}$$

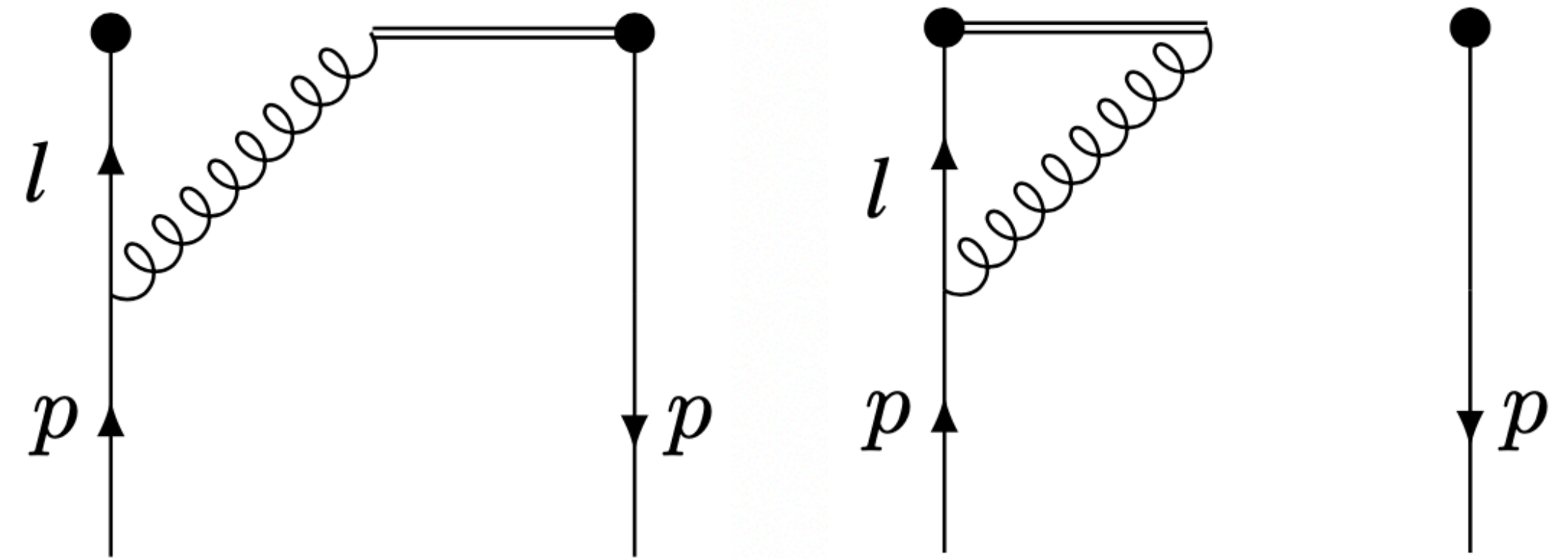
Here the factor $(1-x)^{-2\epsilon}$ is crucial to reproduce the correct sign of leading threshold logarithm, which plays a similar role as the phase-space measure in DIS and DY cross sections.

By expanding in ϵ , we can reproduce the leading threshold logarithm.

22 Origin of threshold logarithms

Leading divergence in the one-loop diagram

$$\begin{aligned} & \tilde{q}_{CS}^{(1)}(x, \vec{k}_\perp, p^z) \\ &= \frac{g^2 \mu^{2\epsilon} C_F}{2(2\pi)^{d-1}} \int_0^1 ds \frac{(1-s)^{2-d}}{\vec{k}_\perp^2} \quad k_t^2 = \vec{k}_\perp^2 / p_z^2 \\ & \times \left[\frac{k_t^2(1+x-2s) + (x-s)^3}{(k_t^2 + (s-x)^2)^{3/2}} - \frac{k_t^2(1+x-2s) + (x-1)^3}{(k_t^2 + (x-1)^2)^{3/2}} \right] \end{aligned}$$



• To obtain the pseudo-PDF

$$\begin{aligned} & \lim_{x \rightarrow 1} \tilde{q}_{CS}^{(1)}(x, \vec{b}_\perp, p^z = \infty) \\ &= \frac{g^2 C_F}{8\pi^2} \Gamma(-\epsilon) \frac{2(1-x)^{2\epsilon}}{(1-x)} (b_\perp^2 \mu^2)^\epsilon \end{aligned}$$

Since the factorization for the pPDF in the small b_\perp limit, the physical scale in the threshold logarithm is proportional to $(1-x)^{-2} b_\perp^{-2}$, which approaches the UV fixed point in the $x \rightarrow 1$ limit.

By expanding in ϵ , we can reproduce the leading threshold logarithm.